



# The insecticide fipronil affects the physical properties of model membranes: A combined experimental and molecular dynamics simulations study in Langmuir monolayers

Iván Felsztyna, Mariela E. Sánchez-Borzone, Virginia Miguel\*, Daniel A. García\*

Universidad Nacional de Córdoba, Facultad de Ciencias Exactas, Físicas y Naturales, Departamento de Química, Cátedra de Química Biológica, Córdoba, Argentina  
 Instituto de Investigaciones Biológicas y Tecnológicas, Consejo Nacional de Investigaciones Científicas y Técnicas, Universidad Nacional de Córdoba, Córdoba, Argentina

## ARTICLE INFO

### Keywords:

Fipronil  
 Gabaergic insecticides  
 Langmuir monolayers  
 Molecular dynamics simulations  
 Drug-membrane interaction

## ABSTRACT

Fipronil is a widely used commercial insecticide whose action mechanism consists in blocking the influx of chloride ions through the  $\gamma$ -aminobutyric acid type A receptor (GABA<sub>A</sub>-R), an integral membrane protein. The present study investigates the interaction of fipronil with phospholipid Langmuir monolayers, in order to characterize the effects that its partition could exert on the physical properties of these model membranes. A combined experimental and molecular dynamics (MD) simulations approach was performed. MD simulations were conducted in such a way that they resemble an experimental compression isotherm of DPPC in the presence of fipronil in the aqueous subphase. Both the experimental and the simulated compression isotherm showed that the partition of fipronil between DPPC molecules induces an expansion of the monolayer. Experimental results also showed that fipronil can penetrate lipid monolayers even in condensed packing states. MD simulations showed that fipronil induces an ordering effect in the acyl chains of DPPC in the liquid-condensed phase. In addition, the simulations indicate that fipronil orients parallel to the plane of the monolayer and that it establishes hydrogen bonds with the glycerol region of DPPC. Free energy profiles of the partition of fipronil into the monolayers, obtained by means of umbrella sampling, indicated that its penetration is thermodynamically favorable, being the interphase between the glycerol region and the acyl chains of DPPC its most favorable location. Our results suggest that fipronil could modulate the supramolecular organization of biological membranes surrounding GABA<sub>A</sub>-R, contributing, at least in part, to its action mechanism.

## 1. Introduction

Phenylpyrazoles constitute a relatively new group of chemical compounds with herbicidal and insecticidal effects. Among them, fipronil (Fig. 1) is a widely used commercial insecticide developed in the eighties and released to the market in 1993 [1]. It has a high activity and a broad spectrum against insect pests and a relatively low toxicity for mammals [2]. Fipronil acts as a potent disruptor of the central nervous system of insects by blocking the influx of chloride ions through the  $\gamma$ -aminobutyric acid type A receptor (GABA<sub>A</sub>-R) [3].

GABA is the major inhibitory neurotransmitter in both vertebrate and invertebrate nervous systems [4]. Its specific target, the GABA<sub>A</sub>-R, belongs to the family of pentameric ligand gated ionic channels (pLGICs). Each of the five subunits of the pLGICs includes a large extracellular domain and four  $\alpha$ -helical transmembrane domains. GABA<sub>A</sub>-R presents allosteric sites that are recognized by many drugs other than

GABA, like benzodiazepines, barbiturates, neuroactive steroids and anesthetics [5]. A site located inside the GABA<sub>A</sub>-R pore in the transmembrane region is the target for many chemically diverse insecticides that block the channel, acting as non-competitive antagonists (NCAs), like fipronil [6]. Fipronil is part of the second generation of GABA<sub>A</sub>-R NCAs, given that it emerged as a much less toxic alternative after the classical organochlorine insecticides, like lindane and dieldrin [7].

Considering that GABA<sub>A</sub>-R is an integral membrane protein, it is known that its activity can be modulated by surface-active compounds and by changes in the physical properties of the lipid membrane [8,9]. Lipophilic compounds that bind to different sites of GABA<sub>A</sub>-R, like benzodiazepines and gabaergic phenols or ketones, interact with both artificial and natural membranes and affect properties like surface curvature, fluidity, acyl chain order and molecular packing [10–16]. Thus, the activity of these gabaergic compounds could be the combined result of their specific binding to the protein and their non-specific

\* Corresponding authors at: Universidad Nacional de Córdoba, Facultad de Ciencias Exactas, Físicas y Naturales, Departamento de Química, Cátedra de Química Biológica, Córdoba, Argentina.

E-mail addresses: [vmiguel@conicet.gov.ar](mailto:vmiguel@conicet.gov.ar) (V. Miguel), [dagarcia@unc.edu.ar](mailto:dagarcia@unc.edu.ar) (D.A. García).

<https://doi.org/10.1016/j.bbamem.2020.183378>

Received 8 April 2020; Received in revised form 21 May 2020; Accepted 22 May 2020

Available online 25 May 2020

0005-2736/ © 2020 Published by Elsevier B.V.

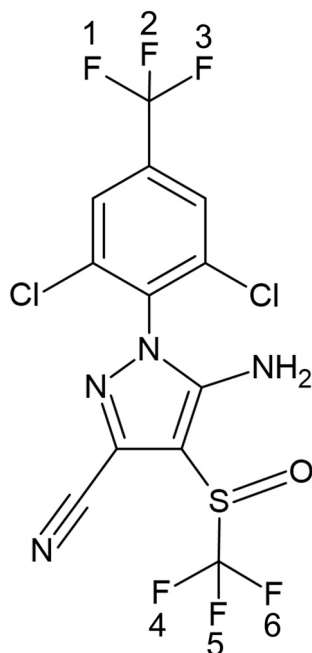


Fig. 1. Chemical structure of fipronil.

interactions with the surrounding lipid molecules, with the subsequent modulation of GABA<sub>A</sub>-R supramolecular environment.

Less is known about the non-specific modulation that insecticidal GABA<sub>A</sub>-R NCAs could produce in the membrane. For instance, some studies conducted to characterize the partition into lipidic phases of the organochlorine lindane, have demonstrated that it can affect the membrane fluidity [17–19]. In the case of fipronil, although several studies were performed in recent years about many of its properties such as its specific interactions with GABA<sub>A</sub>-R, toxicology, environmental fate and selectivity [20–25], the interaction of this highly lipophilic compound with lipid membranes and the possible implications in its action mechanism have not been analyzed yet.

Self-assembled lipid structures mimicking cell membranes, like liposomes, solid-supported membranes and Langmuir monolayers (LM), have been extensively used as experimental models to study the effects of the interaction with bioactive molecules. Many crucial phenomena that take place in bilayers can be elucidated by using monolayers at the air-water interface [26], representing the first contact of lipophilic compounds with plasma membranes. Moreover, phospholipid monolayers constitute simple models to study intermolecular interactions [27,28], given that the lipid interface can be easily modulated by changing the lateral packing using the barriers of a Langmuir trough. As the monolayer is compressed or expanded, lipids explore different phases and undergo a series of phase transitions that manifest themselves on the shape of the lateral-pressure/area isotherm, along with changes in the interfacial electrostatic potential and the reflectivity of the liquid surface [29]. Given that these properties are sensitive to the subphase composition, LM offer a distinctive advantage for sensing drug-lipid interactions [29].

Molecular dynamics (MD) simulations provide an atomic resolution description of the system behavior that can complement the interpretation of experimental trends and data. In particular, MD simulations have been extensively used to analyze phospholipid LM at atomistic and coarse-grained levels of detail being able to reproduce, with varying degrees of accuracy, the rheologic and electrostatic properties of these systems [30–34]. In addition, several computational studies have analyzed the effects of the interaction of drugs [35–37], peptides [38,39], amino acids [29] and ions [40] with phospholipid LM.

The aim of this work is to describe how the penetration of the

gabaergic insecticide fipronil affects the biophysical properties of 1,2-dipalmitoyl-sn-glycero-3-phosphocholine (DPPC) LM. These effects were analyzed by two complementary approaches: i) experimental studies: surface tension-area and surface potential-area compression isotherms, Brewster angle microscopy (BAM) and penetration isotherms and ii) molecular dynamics simulations of DPPC LM in the presence of fipronil at different molecular packing states of the phospholipid.

## 2. Materials and methods

### 2.1. Materials

Fipronil (informed purity  $\geq 95\%$ , checked by GC–MS) was kindly provided by Chemotecnica S.A. (Argentina). 1–2-Dipalmitoyl-sn-glycero-3-phosphocholine (DPPC) lipid was purchased from Avanti Polar Lipids (Alabaster, AL, USA). All other reagents were of the highest analytical grade. Solutions were prepared in bidistilled-deionized water.

### 2.2. Langmuir monolayers

#### 2.2.1. Surface pressure ( $\pi$ )–mean molecular area (MMA) and surface potential ( $\Delta V$ )–MMA isotherms

Compression isotherms were performed for DPPC using a Minitrough II (KSV Instruments Ltd., Finland). Phospholipid monolayers were prepared on the air-water interface by spreading a chloroformic solution of DPPC on the aqueous surface of a Teflon™ trough filled with bidistilled-deionized water. After 5 min of solvent evaporation, the film was compressed isometrically at a constant rate of  $5 \pm 1$  mm/min by means of two barriers moving synchronously. Surface pressure ( $\pi$ ) was measured with a platinum plate by the Wilhelmy plate method [41] and the surface potential ( $\Delta V$ ) was measured by the vibrating plate method (Spot Tune – KSV Ltd.) [42]. DPPC isotherms were determined in the absence and in the presence of fipronil in the aqueous subphase. In the last case, before the formation of the monolayer, fipronil was mixed with the aqueous subphase at four final concentrations: 0.25, 2.5, 25 and 50  $\mu\text{M}$ . Control isotherms obtained in the presence of DMSO 0.25% (v/v) (used as fipronil solvent) were not different from those at 0% DMSO (data not shown). The mean molecular area (MMA) reported is the total monolayer area divided by the total number of DPPC molecules at the interface. For preliminary tests, fipronil solutions dissolved in chloroform were spread alone on the air-water interface in order to test the possible surface activity of this compound. All experiments were carried out at a controlled room temperature (25 °C) and conducted at least three times to assure reproducibility. For each isotherm, one representative curve is shown.

To analyze more deeply the phase behavior of the films, the compressibility modulus (K) was obtained for each system. K values represent the reciprocal of the compressibility and were calculated from  $\pi$ -MMA isotherms applying Eq. (1) [43]:

$$K = -MMA_{\pi} \left( \frac{d\pi}{dMMA} \right)_T \quad (1)$$

#### 2.2.2. Penetration of fipronil into DPPC monolayers

In order to study the ability of fipronil to penetrate into DPPC monolayers, the experiments were performed in a circular home-made Teflon trough (15 ml volume) containing bidistilled-deionized water as subphase. Increasing volumes of a chloroformic DPPC solution were spread on the interface in order to form monolayers at different initial  $\pi$  ( $\pi_i$ ). Fipronil was injected into the subphase from a stock solution of DMSO to a final concentration of 50  $\mu\text{M}$ . The injection was done after the stabilization of the  $\pi_i$  of the film (between 5 and 10 min), at  $25 \pm 1$  °C. These experiments were performed under continuous

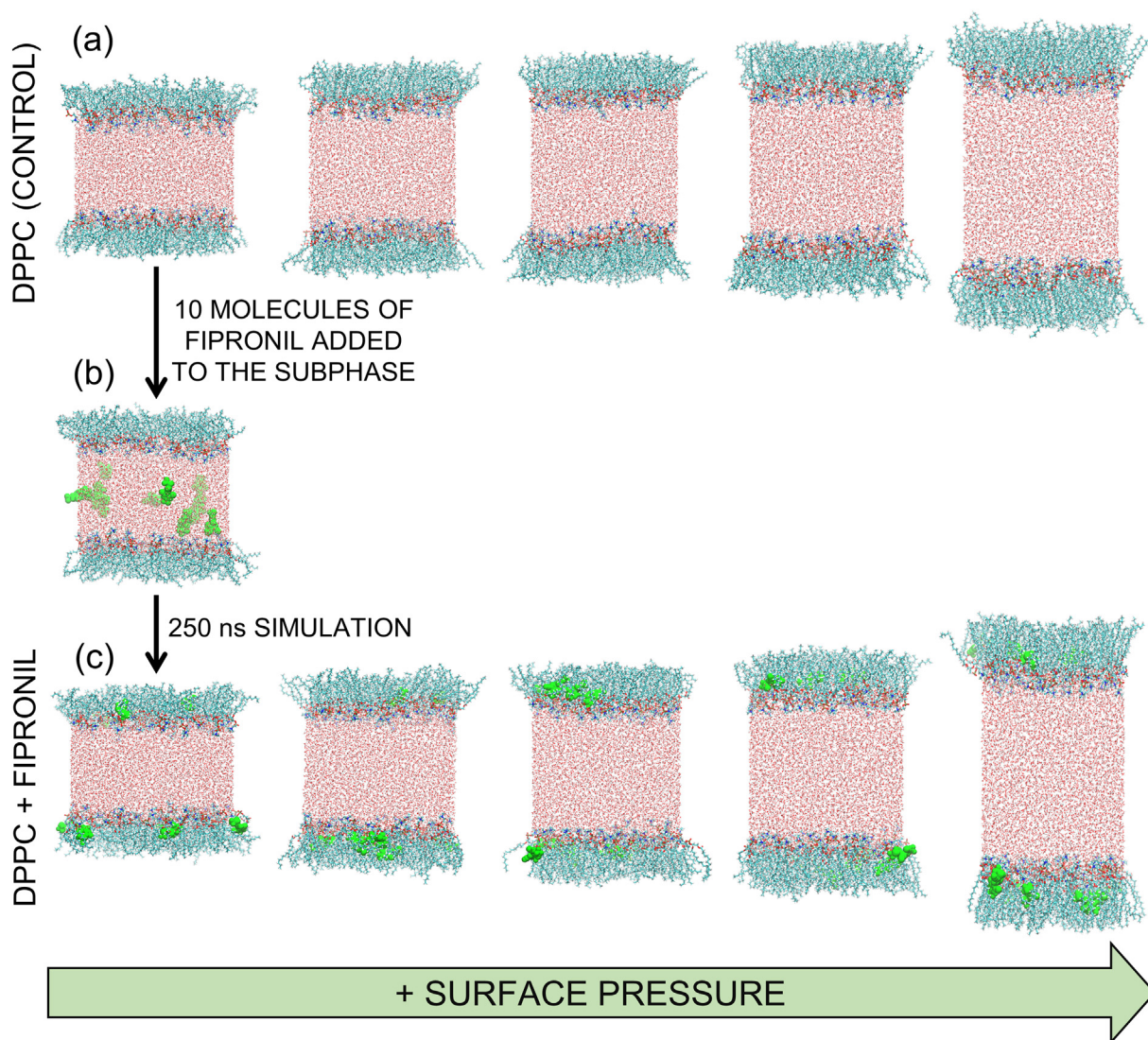


**Fig. 2.** Snapshots of the simulated systems showing the simulation protocol used. Liquid-expanded DPPC monolayers were equilibrated for 150 ns in a pure water subphase (a). In the final configuration of this system, ten molecules of fipronil (shown in green) were added to the subphase (b). This new system was simulated for 250 ns and all the molecules of fipronil spontaneously partitioned into the monolayers (c). To the final configuration of the system in (c) several successive surface tension values were imposed, in order to obtain a simulated compression isotherm. In each case, the final configuration of the previous run was used as the starting point for the next simulation. The same surface tension values were used to simulate the control systems (pure DPPC). (For interpretation of the references to color in this figure legend, the reader is referred to the web version of this article.)

stirring (150–250 rpm).  $\pi$  vs. time was recorded at constant surface area in order to measure the increment in  $\pi$  induced by the penetration of the insecticide into preformed DPPC monolayers, until equilibrium  $\pi$  were reached (changes in  $\pi < 1$  mN/m per hour). Finally, plots of  $\Delta\pi$  vs.  $\pi_i$  were graphed to determine the  $\pi_{\text{cut-off}}$  for fipronil, meaning the maximum  $\pi$  at which the insecticide would be able to penetrate the monolayer.

### 2.2.3. Brewster angle microscopy (BAM)

The Langmuir equipment was mounted on the stage of a Nanofilm EP3 imaging Ellipsometer (Accurion, Göttingen, Germany), which was used in the Brewster Angle Microscopy (BAM) mode. Minimum reflection was set with a polarized 532 nm laser incident on the bare aqueous surface at the experimentally calibrated Brewster angle ( $\sim 53.1^\circ$ ). DPPC compression isotherms were visualized in the absence and in the presence of 25  $\mu\text{M}$  fipronil dissolved in the aqueous subphase. After DPPC monolayer formation, and during compression, the reflected light was collected with a 20 $\times$  objective and an analyzer-polarizer lens connected to a CCD camera. For a better visualization, the lower

0–100 Gy level range (from the 0–255 original scale) was selected using the free software ImageJ 1.51q [44].

### 2.3. Molecular dynamics simulations

Equilibrium MD simulations and Potential of Mean Force (PMF) calculations were carried out in GROMACS v.2018.6 with GPU acceleration [45]. The All Atom (AA) Slipids force field [46] was used for lipids and the TIP3P model for water molecules [47].

The construction of fipronil units to be used in MD simulations was made with the AnteChamber module, using the protocol described before [48]. Quantum chemical calculations of the optimized structure and RESP charges were obtained as before [48] with the Gaussian 03 package [49]. Fipronil units were obtained using the GAFF force field [50]. The AnteChamber Python Parser interface (ACPYPE) [51] was employed to translate the parameter files to be used with GROMACS code.

The simulated systems consist of cells containing 128 DPPC molecules divided into two monolayers with 64 molecules each. The initial



system was built in a cubic box, using the Packmol package [52]. The monolayers are separated by a slab containing  $\sim 8600$  water molecules. Periodic boundary conditions were used along the X, Y and Z directions. No interactions between the monolayers are expected across the Z direction because of the large vacuum regions and the large size of the water slab, as shown in Fig. S1. The total length of the Z axis of the simulation box is 27 nm. The simulated system geometry is similar to that proposed by Feller et al. [53,54], and was used in many studies [34,36].

The simulations were carried out in the  $N\gamma P_z T$  ensemble, being N the number of particles, T the temperature (298 K),  $P_z$  the normal component of the pressure tensor (1 bar), and  $\gamma$  the surface tension [29]. This ensemble maintains a constant Z dimension, while the X and Y dimensions are allowed to adjust in response to an imposed surface tension [29]. Surface tension in MD simulations ( $\gamma_{MD}$ ) is calculated from the lateral and tangential components of the pressure tensor:

$$\gamma_{MD} = L_z(P_{zz} - 0.5(P_{xx} + P_{yy}))$$

where  $L_z$  is the length of the simulation box in the direction perpendicular to monolayers,  $p_{zz}$  is the pressure normal to monolayers,  $p_{xx}$  and  $p_{yy}$  are pressure values in the directions parallel to the monolayers [34]. With this simulation setup, the surface pressure ( $\pi_{MD}$ ) was obtained from

$$\pi_{MD} = \gamma_w - \gamma_m$$

where  $\gamma_w$  is the surface tension of the TIP3P water at 298 K [55], and  $\gamma_m$  is the calculated surface tension of the monolayer. The area per lipid (APL) is calculated using the area of the simulation box (x and y axes) divided by the number of lipids per leaflet.

Several unbiased simulations were carried out in order to reconstruct surface pressure-area isotherms in the absence and in the presence of fipronil. Firstly, a liquid-expanded DPPC monolayer ( $\pi \approx 0$ ) was equilibrated in a pure water subphase. Subsequently, 10 molecules of fipronil were randomly located into the water solvent and the overlapping water molecules in a ratio of 2 Å were removed. The DPPC/fipronil ratio (128:10) in this system is comparable with the one that corresponds to the 25  $\mu\text{M}$  fipronil concentration used in our experiments. This system was subjected to a steepest descent energy-minimization followed by a 250 ns  $N\gamma P_z T$  MD simulation in which fipronil molecules partitioned into the phospholipid monolayers (Fig. 2). The resulting configuration was then used as the starting configuration for another simulation with a different surface pressure value (9.9 mN/m). This procedure, consisting of using the previous run as the starting point for the next simulation, was repeated with three different surface pressures (12.8, 18 and 39.8 mN/m). The same parameters were imposed to the neat DPPC monolayers, and these simulations were used as controls for the subsequent analysis. All the simulations in the presence of fipronil were performed for 250 ns (300 ns in the case of the most compressed system) while the control systems were simulated for 150 ns. In the former, the last 100 ns were considered for the analysis, while in the latter the last 50 ns were used. The convergence of the interfacial area was used as the criterion of a proper equilibration of the systems.

The Berendsen algorithm was used for the thermostat and the barostat [56], with time constants of 0.1 and 1 ps, respectively. All chemical bonds were constrained using LINCS algorithm. Constraining the bond lengths allowed to use a time step of 2 fs. The Lennard-Jones interactions were truncated at 1.0 nm. The particle mesh Ewald method [57] was used to evaluate the electrostatic interactions, with a real-space cutoff of 1.0 nm.

PMF simulations were carried out in the equilibrated systems with pure water subphase obtained from the simulations described before. Two calculations were performed, one in the most expanded state and the other one in the most condensed state. One fipronil molecule was placed in the middle of the water slab and was pulled into the monolayer, that is, along the z-axis of the simulation box. PMF was calculated

as a function of the distance of the center of mass of the fipronil molecule and the center of mass of one of the monolayers. A series of 20 separate simulations of 60 ns each were performed, in which the fipronil molecule was restrained in the z-coordinate by a harmonic restraint. A force constant of 1000  $\text{kJ}\cdot\text{mol}^{-1}\cdot\text{nm}^{-2}$  was used. The Weighted Histogram Analysis Method (WHAM) was used to extract the PMF and calculate  $\Delta G$  [58]. The error bars for these calculations were obtained using the bootstrap method [59].

The visualization of the simulation trajectories and the snapshots of the different simulated systems were conducted in VMD [60].

### 3. Results and discussion

#### 3.1. Surface pressure-area and surface potential-area isotherms

When fipronil was spread alone on the air-water interface and compressed until the minimum area allowed by the Langmuir trough, no change in the surface pressure was observed (results not shown). This result indicates that fipronil is not able to form stable Langmuir monolayers by itself [61]. Therefore, the effects of fipronil on the DPPC compression isotherm can be interpreted as a consequence of its interactions with the phospholipid molecules.

Fig. 3 (upper panel) shows  $\pi$ -MMA compression isotherms of DPPC in the absence (control) or in the presence of three increasing concentrations of fipronil previously dissolved in the aqueous subphase (0.25, 2.5 and 25  $\mu\text{M}$ ). The pure DPPC monolayer isotherm is similar to that obtained in previous studies [62,63]. The plateau below 10 mN/m corresponds to the liquid expanded-liquid condensed coexistence

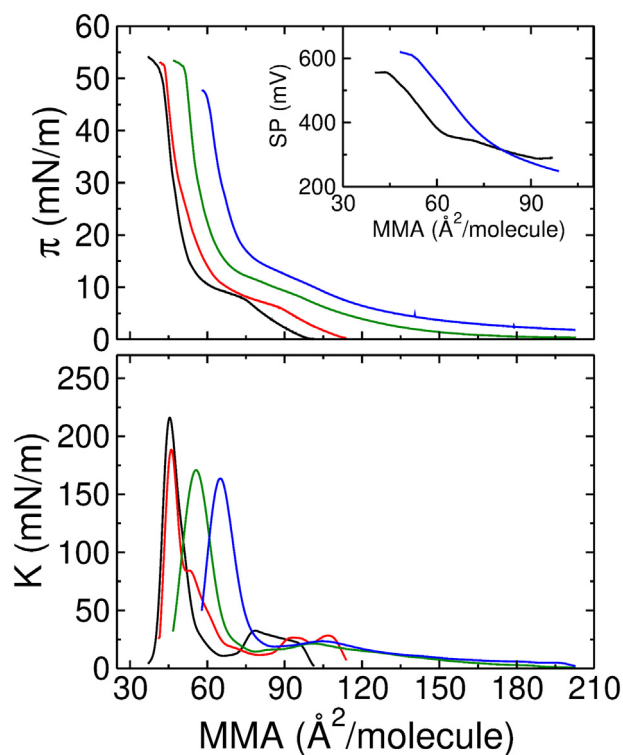


Fig. 3. (upper panel)  $\pi$ -MMA compression isotherms of DPPC. Isotherms in the absence (black line) and in the presence of three increasing concentrations of fipronil previously dissolved in the aqueous subphase: 0.25  $\mu\text{M}$  (red line), 2.5  $\mu\text{M}$  (green line) and 25  $\mu\text{M}$  (blue line). The inset plot shows SP-MMA compression isotherms of DPPC in the absence (black line) and in the presence of 25  $\mu\text{M}$  fipronil (blue line). The SP-MMA isotherm in the presence of fipronil was cut at  $\text{MMA} \sim 100 \text{ \AA}^2$  to clarify the visualization. (lower panel) Compressibility modulus (K) vs. MMA. The values were calculated from the  $\pi$ -MMA isotherms. (For interpretation of the references to color in this figure legend, the reader is referred to the web version of this article.)

region (LE-LC), and the subsequent sharp increase of  $\pi$  represents the LC phase [63].

In the presence of fipronil, the isotherms are shifted to larger areas in a concentration-dependent manner. This expansion of the DPPC isotherm reflects the fact that fipronil molecules partition into the lipidic phase, occupying area in the interface and acting as spacers between the phospholipid molecules [64]. The isotherm conducted on a subphase with 50  $\mu\text{M}$  fipronil overlaps with the 25  $\mu\text{M}$  curve (results not shown), indicating that, at this concentration, the monolayer saturates in terms of the incorporation of fipronil molecules.

Surface potential (SP)-MMA compression isotherms (upper panel — inset plot) were conducted for DPPC in the absence and in the presence of 25  $\mu\text{M}$  fipronil. The SP is a measure of the vertical component of the electrostatic field across the lipid/aqueous interface and its variation is typically associated with a change in the phospholipid molecular orientation [65]. In the LC phase, DPPC monolayers have large SP values because the interactions between neighboring molecules are maximized, while in the LE phase the molecules are less packed, less ordered and with more tilted alkyl chains, resulting in lower surface potentials [65]. It can be observed that in the LC region of the isotherm the SP increases in the presence of fipronil, reaching a higher value at the collapse in comparison to the control isotherm. The possible factors influencing this behavior will be further analyzed in light of the MD simulations results.

The lower panel in Fig. 3 depicts K-MMA curves calculated from  $\pi$ -MMA isotherms. K reflects the physical state of the monolayer. The higher the K values, the lower the interfacial elasticity [12]. In the presence of fipronil, K values tend to decrease with respect to the control curve, indicating that fipronil increases the elasticity of the DPPC monolayer. The decrease of K values is reported in the literature for other drugs interacting with lipid LM and could be a consequence of a compressional gain of the film owing to the fact that the rigid structure of the well-packed phospholipid monolayer is smoothed by the presence of fipronil [64].

In addition, a maximum in the K-MMA curve indicates the onset of the phase transition. In the presence of 2.5 and 25  $\mu\text{M}$  fipronil, the LE to LC phase transition initiates at higher surface pressures and at higher molecular areas. The transition becomes less defined in comparison to the isotherm of pure DPPC. This result points to a non-first order transition as a consequence of the molecular interactions between the phospholipids and fipronil [66]. These effects in the phase transition are more pronounced as the concentration of fipronil increases. Therefore, the insecticide favors the liquid-expanded phase in a concentration-dependent manner.

The collapse surface pressure ( $\pi_c$ ) is almost unaffected at 0.25 and 2.5  $\mu\text{M}$  fipronil, but it is diminished at 25  $\mu\text{M}$  (Table S1). This indicates that the DPPC monolayer is destabilized at this high concentration of fipronil in the subphase.

It is important to consider that the expanding effect of fipronil in the DPPC monolayer is present through the whole isotherm, even in the LC phase. In fact, the minimum molecular areas reached in the presence of fipronil are higher than in the control isotherm (Table S1). This suggests that fipronil is not expelled from the interface as the molecular packing of the film increases.

### 3.2. Penetration of fipronil in DPPC monolayers at the air-water interface

Fipronil is a lipophilic molecule with a theoretically estimated octanol-water partition coefficient (Log P) of 4.5 [67], which suggests that it has a high affinity for lipidic phases and for interacting with DPPC LM. In penetration experiments, a fixed concentration of fipronil (50  $\mu\text{M}$ ) is injected into the subphase over which a DPPC monolayer is pre-formed. These monolayers are built at different initial surface pressures ( $\pi$ ) and at a constant area. In this way, the increase in  $\pi$  ( $\Delta\pi$ ) after the injection is interpreted in terms of the penetration of fipronil into the lipid monolayer. Penetration of small molecules has been

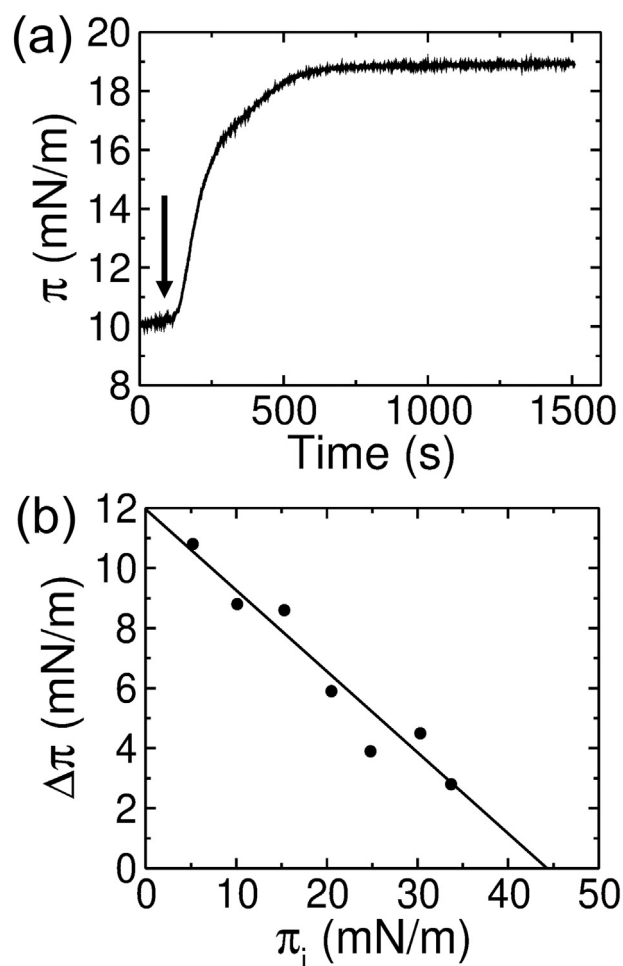


Fig. 4. Fipronil penetration into DPPC monolayers. (a) A typical curve showing the increase in  $\pi$  ( $\Delta\pi$ ) as a function of time after the injection of fipronil in the subphase. The time of the injection is marked with an arrow. (b)  $\Delta\pi$  vs. initial surface pressure ( $\pi_i$ ) of different penetration experiments and linear regression of the data.

reported in the literature for other drugs [68] and for peptides [69]. In all cases, an increase in the surface pressure indicated the penetration of the compound into the lipidic phase [66].

A typical curve from these experiments is depicted in Fig. 4a, which shows the variation in  $\pi$  as a function of time at a  $\pi_i$  of 10 mN/m after the injection of 50  $\mu\text{M}$  fipronil in the subphase. The surface pressure increases abruptly due to fipronil penetration in the monolayer and reaches a plateau at a value  $\sim 8$  mN/m higher. The stability of the plateau suggests that once the compound penetrates in the lipidic phase, it is not expelled to the subphase.

Fig. 4b shows the variations of  $\pi$  ( $\Delta\pi$ ) caused by the penetration of fipronil as a function of the initial  $\pi$  ( $\pi_i$ ) of the DPPC monolayer. It can be observed that the insecticide is able to penetrate the monolayer in a wide range of  $\pi_i$ , even in the LC phase. However, as could be expected, the changes in  $\pi$  are less pronounced as the monolayers are more tightly packed. The data was fitted with a linear regression ( $r^2 = 0.94$ ;  $p < 0.0001$ ), from which the maximum  $\pi$  allowing fipronil penetration ( $\pi_{\text{cut-off}}$ ) was determined to be 44.3 mN/m. This value is much higher than the average lateral pressure estimated for a natural lipid bilayer (30–35 mN/m) [70,71], so fipronil is expected to incorporate favorably in cell membranes.

### 3.3. Brewster angle microscopy of DPPC monolayers

Brewster angle microscopy (BAM) allows to visualize the phase

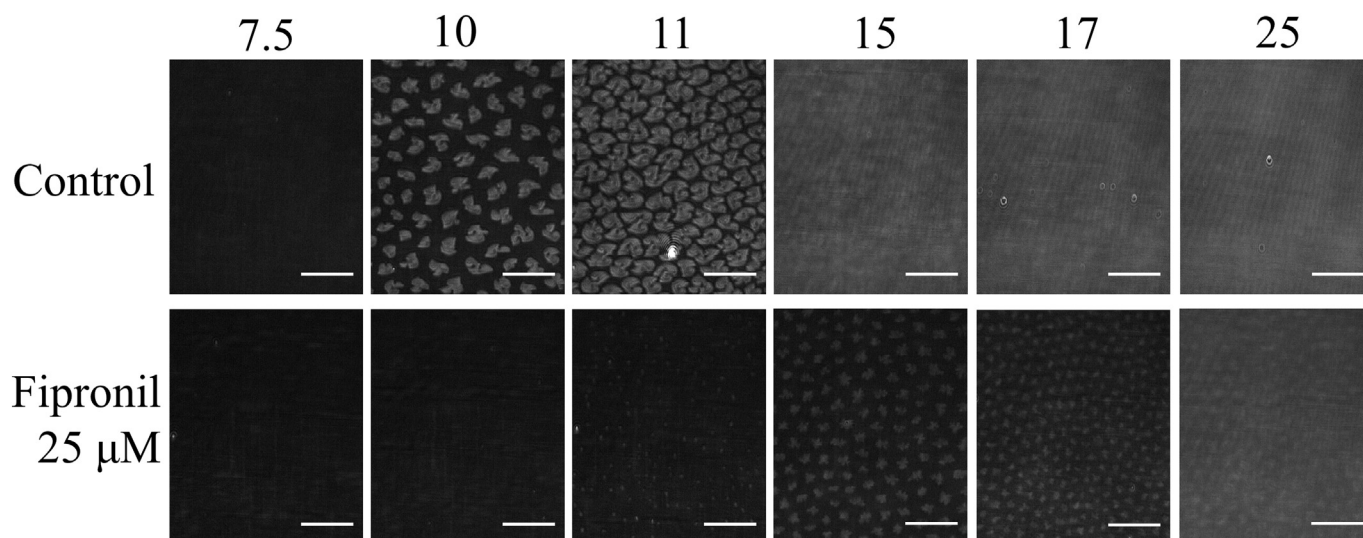


**Fig. 5.** Brewster angle microscopy visualization of DPPC monolayers. The images correspond to monolayers in the absence (upper panels, Control) and in the presence of 25  $\mu\text{M}$  fipronil in the subphase (lower panels). Monolayers were compressed at a rate of 5 mm/min. The numbers above the images indicate the corresponding surface pressures (in mN/m). Representative images were taken from two independent experiments. White bars represent 50  $\mu\text{m}$ .

behavior of a monomolecular layer throughout its compression. The possible changes that lipophilic drugs can cause in the size and shape of DPPC LC domains can be analyzed. BAM images of a pure DPPC monolayer (Fig. 5, upper panels) show the LC domains as brighter structures during the phase transition, with their characteristic shape curving in a counterclockwise direction, as expected for L-DPPC [12].

In the presence of 25  $\mu\text{M}$  fipronil in the subphase (Fig. 5, lower panels), the LC domains appear later in the compression isotherm and the LE-LC coexistence persists until higher  $\pi$ , effects that were also observed in the analysis of the  $\pi$ -MMA isotherm (Section 3.1). The LC domains become smaller and they lose their characteristic shape, presenting a starry structure.

Since DPPC is a chiral molecule, microscopic studies of phospholipid domains in monolayers on the aqueous surface allow to observe the effect of this optical isomerism on the curvature of LC domains. In this case, the clockwise or counterclockwise curvatures of the triskelion of DPPC are directly related to the absolute configuration of the enantiomer on those domains [72,73]. The loss of chiral shapes in the LC domains in the presence of fipronil would indicate its interaction with phospholipid molecules affecting the head group region and modifying the molecular array as was previously described for other compounds [12,13]. Molecular studies of dipolar repulsion in monolayers have demonstrated that a small change in the charge distribution of the polar region could be transduced to changes in domain size and shape [74]. Thus, it is expected that the partition of fipronil between the phospholipid molecules would modify the dipolar arrangement of the chiral DPPC in the tilt direction, allowing the LC domains to grow in different directions.

### 3.4. All atom equilibrium MD simulations

DPPC monolayers were simulated in the presence and in the absence of fipronil in the aqueous subphase, at different molecular packing states. In the first set of simulations, a DPPC monolayer in the LE phase was simulated for 150 ns. To the final configuration of this system, ten molecules of fipronil were added in the subphase, and this new system was simulated for 250 ns. The diffusion of fipronil inside the monolayer was assessed along the MD. At 16 ns, six fipronil molecules were found inside one of the monolayers and the other four molecules partitioned into the other one, remaining inside the lipidic phase along the entire time of the simulation (Fig. S2-a). This system, with the molecules of fipronil already equilibrated inside the DPPC monolayer, was simulated

at different surface tension values in order to obtain a simulated compression isotherm and be able to compare it with the experimental data. It is remarkable that in all the simulations obtained from the compression of the first system, the fipronil molecules remained inside the monolayer, surrounded by the DPPC molecules (Fig. S2).

Fig. 6 depicts the simulated surface pressure-area isotherm for DPPC in the presence and in the absence of fipronil in the subphase, at a temperature of 298 K. The control isotherm presents a general agreement with the experimental data regarding the range of area per lipid (APL) and surface pressure covered by the curve. The observed discrepancies are similar to those typically obtained in MD simulations of lipid monolayers [34,75]. Although a change in the slope of the isotherm can be observed at  $\sim 10$  mN/m, the region of first order phase transition, characteristic of the DPPC isotherm, could not be observed. The lack of a clear LE-LC coexistence may be caused by the limited size

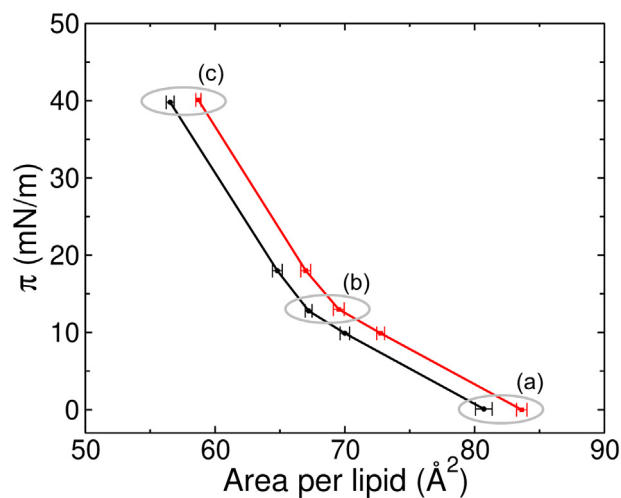


**Fig. 6.** Simulated  $\pi$ -area isotherm for DPPC monolayers at 298 K on pure water (black points), and in the presence of ten molecules of fipronil (red points). The lines joining the points are just a guide to the eye. The points enclosed by grey ellipses correspond to the systems used for subsequent analysis of the effects of fipronil on the LE (a), LE-LC (b) and LC (c) phases of DPPC. The error bars in the area per lipid were calculated by block averaging and correspond to 95% confidence intervals. (For interpretation of the references to color in this figure legend, the reader is referred to the web version of this article.)



of the simulation box, as reported previously by other authors [33,34]. Although more accurate quantitative results were obtained by simulating LM with the four point OPC water model [76], we decided to use the TIP3P water given that this is the original combination in which the Slipids force field was parameterized [46]. Anyway, a quantitative level of detail in the simulated DPPC isotherm is not the aim of this study. Conversely, we focus on the exploration of the effects that a drug, in this case fipronil, produces when it interacts with DPPC monolayers.

In that sense, it is clear from Fig. 6 that the addition of fipronil to the subphase produces a significant shift of the isotherm to larger areas. This is consistent with the trend observed in the experimental isotherm. We can confirm from the MD simulation that fipronil molecules partition into the lipidic phase and act as spacers between DPPC molecules, increasing the area per lipid.

Three points in the isotherm were selected to perform further analysis about the effects that fipronil produces in the phospholipid monolayer. These systems were chosen in order to analyze three different packing states of the phospholipid that, according to their surface pressure values, would correspond to the LE, LE-LC and LC phases in the experimental isotherm. The assignment of each system to each of these phases is based not only on their positions in the simulated isotherm, but also in the chain-chain radial distribution function (RDF) (Fig. S3) and in the visual inspection of the trajectories (Fig. 2). The RDF reaches higher values for DPPC monolayers in the condensed state (lower surface area per lipid) than in the expanded phase (higher surface area per lipid). This result is clearly related to the increasing packing of lipids associated with lipid compression [40]. The liquid condensed phase is characterized by the existence of long-range order in the RDF, that is lost below the suggested phase transition [30]. Fig. S4 shows the RDF profiles between the phosphate groups in the neat DPPC monolayers and in the same systems in the presence of fipronil. Although slight, the decrease of the peaks in the profiles of the LE-LC system in the presence of fipronil gives an idea of a disordering effect in the disposition of the polar head groups that could explain the changes in the shape and size of LC domains during the phase transition that were observed in BAM experiments.

The location of a lipophilic compound within the membrane is extremely important to determine the effects it could exert, especially in drugs whose target are membrane proteins [77]. In MD simulations studies, drug location can be observed directly from density profiles or from free energy profiles of the drug partition [77].

Fig. 7 shows the density profiles obtained along the normal to the membrane plane (*z* axis) of different regions of the DPPC molecules, as well as the density of fipronil molecules. A comparison of the profiles of pure DPPC (upper panels) and the profiles of the monolayers in the presence of fipronil (lower panels) indicates that fipronil molecules are predominantly found in the interphase between the glycerol group and the hydrocarbon chains of DPPC. It can be observed that as the monolayer is more tightly packed, fipronil occupies a slightly deeper position in the monolayer. The location of fipronil indicates that it could produce changes in the structure and dynamics of the acyl chains of DPPC.

The lipid tail order parameter is a standard quantity that allows to evaluate the structural order of acyl chains in lipid monolayers and bilayers, which can be obtained experimentally from deuterium NMR measurements [36]. In MD simulations it is defined by:

$$S_{CD} = \left\langle \frac{3}{2} \left( \cos^2 \Theta - \frac{1}{2} \right) \right\rangle$$

where  $\Theta$  is the angle formed between the C–H bond and the normal of the lipid monolayer, and the angular brackets represent the average over time and over all lipids [77].

The order parameter is related to the tilt angle of the chains and to trans-gauche distribution of chain dihedrals, but the relationship is indirect [78]. Fipronil produces a significant ordering effect in the

acyl chains in the LE-LC and the LC phases, more precisely in the region of the carboxylic atoms of the glycerol skeleton (Fig. 8). The ordering of acyl chains is more relevant as the molecular packing increases. The employment of the NP<sub>*z*</sub>T ensemble for these MD simulations assures that this ordering effect in the acyl chains is effectively caused by the interaction of fipronil with DPPC molecules, and not an artifact of the ensemble, as could occur in the case of NVT simulations of monolayers, where the simulation box is not allowed to expand in response to the partition of a surface active molecule in the interphase.

When DPPC-DPPC Lennard-Jones (LJ) interactions were analyzed in both condensed and expanded phases in presence or in absence of fipronil, no differences were observed (data not shown). Therefore, the increase in the order parameter is not due to fipronil inducing more interactions among the alkyl chains of DPPC. Instead, this effect could be caused by the reduction in the rotational freedom of the acyl chains caused by the presence of fipronil molecules in that region of the monolayer, being more pronounced in the LC phase. Indeed, the DPPC-Fipronil LJ attractive interactions are more significant in the LC than in the LE phase (not shown).

At this point, it is interesting to revisit the experimental results about the effects of fipronil in the surface potential of DPPC monolayers. According to the Demchak-Fort model, the surface potential of a lipid monolayer can be described as a three-layer capacitor with contributions from the alkyl chains, the headgroups and the oriented water molecules in the vicinity of the headgroups [79]. The surface potential increases when the acyl chains become more ordered and when the polar headgroups orient closer to the surface normal [65]. Our MD simulations show that fipronil would not affect the orientation of the polar headgroups, as shown by the unchanged tilt of the P–N vector with respect to the normal (Fig. S5). Consequently, the increase in DPPC acyl chain order in the LC phase caused by fipronil could be the main contribution to the increase in surface potential observed in the experimental SP-MMA isotherm (Fig. 3). This analysis is also supported by the calculations of the monolayer thickness in the absence and in the presence of fipronil (Table S2). The thickness becomes higher in the presence of fipronil in the LE-LC and in the LC phases. However, an effect on the orientation of the interfacial water dipoles cannot be discarded.

We also studied the time evolution of hydrogen bonds of fipronil, both with water as well as with DPPC. Table 1 depicts the average number of H-bonds between different groups and Fig. S6 shows the time evolution of these interactions. It has to be considered that DPPC does not have any hydrogen donor group and that the –NH<sub>2</sub> group is the only donor of fipronil. So, the different types of H-bonds that can be formed in the simulated systems are those between the acceptor groups of DPPC (phosphate oxygens and carboxylic oxygens of glycerol) and the –NH<sub>2</sub> group of fipronil, the H-bonds between water molecules and the acceptor groups of DPPC and the ones between water molecules and fipronil, including those with the –NH<sub>2</sub> group and the ones with its acceptor groups.

When the total number of hydrogen bonds of fipronil molecules with water was analyzed, a reduction associated with fipronil insertion into the monolayer was observed (Fig. S6, LE phase). The number of H-bonds between fipronil –NH<sub>2</sub> and DPPC increases as the molecular packing increases, and more interactions are formed with glycerol while the H-bonds with the phosphate group decrease. This is consistent with the density profiles and the plots of fipronil distribution along the *z*-axis, that shown that fipronil locates deeper inside the monolayer as it gets more compressed. Although fipronil does not produce by itself a decrease in the number of water molecules establishing H-bonds with DPPC glycerol group, the dehydration of this region that occurs throughout the compression allows fipronil to increase the number of interactions that it establishes with this region of DPPC (Table 2).

To get a deeper insight into the possible orientation that fipronil molecules acquire inside the lipid monolayer, we analyzed the orientation of the principal axis of fipronil with respect to the *z*-axis,

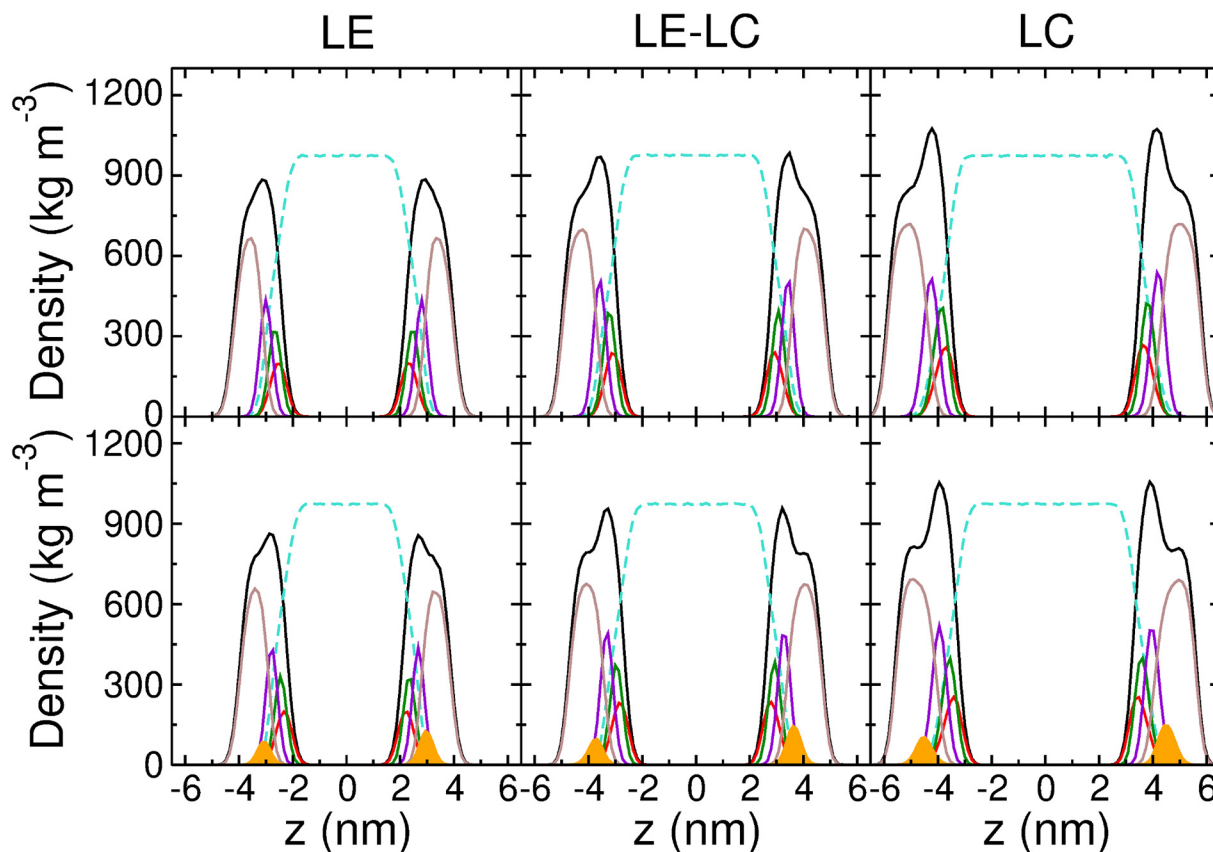


Fig. 7. Density profiles of DPPC monolayers in the LE, LE-LC and LC phases along the z-axis. Upper panels depict the profiles of control systems and the lower panels correspond to the monolayers in the presence of fipronil. The colors represent the different components: DPPC (black line), water (turquoise dashed line), DPPC choline group (red line), DPPC phosphate group (green line), DPPC glycerol group (violet line), DPPC hydrocarbon chain (brown line) and fipronil (orange line, filled to zero). (For interpretation of the references to color in this figure legend, the reader is referred to the web version of this article.)

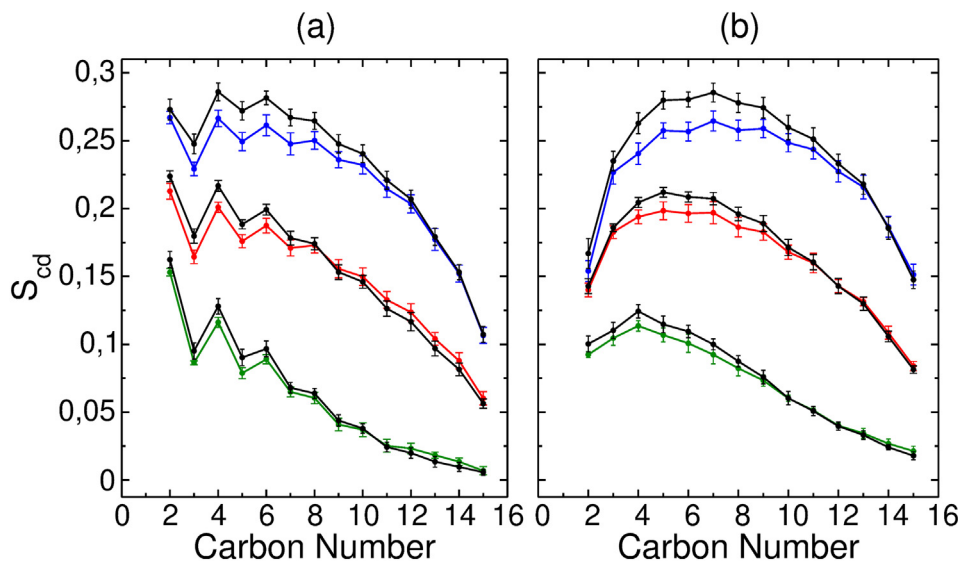


Fig. 8. Deuterium order parameter of the sn-1 (a) and sn-2 (b) hydrocarbon chains of DPPC. Green lines correspond to the LE phase, red lines to the LE-LC phase and blue lines to the LC phase of the control systems. In each case, the black lines correspond to the same system in the presence of fipronil. Error bars were calculated by taking the standard error of the mean for 10 ns windows in the corresponding trajectories. (For interpretation of the references to color in this figure legend, the reader is referred to the web version of this article.)

normal to the monolayer (Fig. 9). It can be observed that the peak of the histogram is centered at  $90^\circ$ , so the most preferable orientation of fipronil consists of the molecule lying parallel to the plane of the monolayer. This could explain the significant increase in the area per lipid, both in the experimental as well as in the simulated isotherms. In addition, it is noticeable that as the compression increases, fipronil molecules tend to orient more vertically, as can be seen by the displacement of the peak of the angle distribution for the LE-LC and the LC

phases. This rearrangement of fipronil orientation inside the monolayer can contribute to the compressional gain of the system, as described above for the experimental compressional modulus ( $K$ ) vs MMA plots.

In order to complement this result, Fig. S7 depicts the time evolution of the minimum distances between some of the atoms of fipronil and different regions of DPPC. As expected from H-bonds analysis, the  $-\text{NH}_2$  group locates close to glycerol and phosphate groups of DPPC and moves away from the phosphate group as the monolayer



**Table 1**  
H-bonds in systems DPPC + FIPRONIL.

	LE		LE-LC		LC	
	Fipronil	Fipronil NH <sub>2</sub>	Fipronil	Fipronil NH <sub>2</sub>	Fipronil	Fipronil NH <sub>2</sub>
H <sub>2</sub> O	18.27 ± 0.22	9.26 ± 0.14	15.46 ± 0.19	8.99 ± 0.13	12.75 ± 0.17	7.50 ± 0.11
DPPC		3.60 ± 0.10		5.11 ± 0.12		5.31 ± 0.12
DPPC glycerol		2.06 ± 0.09		3.13 ± 0.10		4.38 ± 0.11
DPPC phosphate		1.58 ± 0.07		1.97 ± 0.08		0.94 ± 0.07

The values correspond to the average number of H-bonds that the whole molecule of fipronil and its –NH<sub>2</sub> group establish with different regions of DPPC molecules along the time of the simulations.

**Table 2**  
H-bonds between DPPC glycerol and H<sub>2</sub>O.

	LE	LE-LC	LC
DPPC	267.93 ± 0.65	234.27 ± 0.83	207.81 ± 0.82
DPPC + FIPRONIL	267.32 ± 0.62	233.94 ± 0.61	208.52 ± 0.63

The values correspond to the average number of H-bonds between the glycerol group of DPPC and water in the pure DPPC systems and in the systems with fipronil.

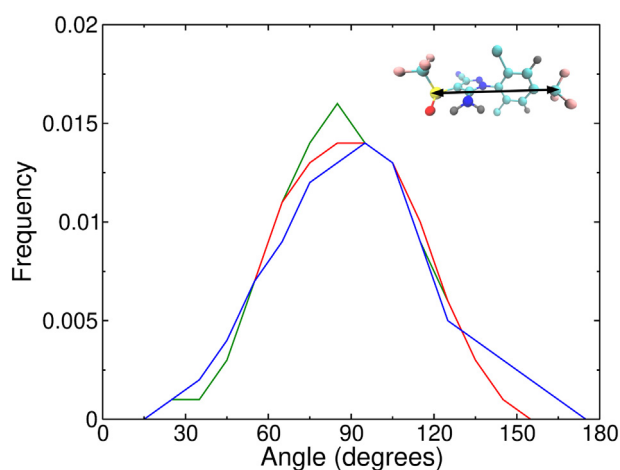


**Fig. 9.** Angle distribution between the principal axis of fipronil and the z-axis of the simulation box in different phases of DPPC LM. LE (green line), LE-LC (red line) and LC (blue line). The inset of the plot shows the defined axis for the fipronil molecule in this calculation. (For interpretation of the references to color in this figure legend, the reader is referred to the web version of this article.)

compresses. The oxygen atom also locates near those groups. Both –CF<sub>3</sub> groups maintain almost the same distances to the different regions of DPPC, as expected from the parallel to the monolayer orientation of the molecule.

### 3.5. Potential of mean force calculation of fipronil penetration into DPPC monolayers

We computed potential of mean force (PMF) calculations to determine the probable distribution of fipronil at different regions of the DPPC monolayer and to gain a thermodynamic insight on the partition of the insecticide into the lipidic phase. Two simulation conditions were considered: one with the monolayer in the LE phase and the other one in the LC phase, in order to analyze the energetics of the penetration of fipronil in both molecular packing states (Fig. 10). Both systems were maintained in the corresponding phase by applying a controlled surface tension, at a temperature of 298 K. Free energy profile calculations were derived from the PMF extracted from a series of umbrella sampling simulations. The curves were aligned so that the fipronil relative

free energy in bulk water corresponds to zero in each case.

The shapes of the free energy profiles in the LE and in the LC phases are similar, both showing a global minimum inside the lipid monolayer. This indicates that the penetration of fipronil into the lipidic phase is highly favorable and explains why fipronil molecules are never expelled from the monolayers during the time of simulation in unbiased MD trajectories. The free energy minimum is located in the interphase between the glycerol group and the acyl chain of DPPC, so this region would correspond to the most favorable location for fipronil inside the monolayer. This coincides with the maximum density of fipronil obtained in unbiased simulations. As described below, the –NH<sub>2</sub> group of fipronil interacts specifically with the oxygen atoms of glycerol, establishing hydrogen bonds, contributing in this way to the favorability of this location for the molecule.

In addition, in both cases the free energy increases until taking positive values while fipronil goes deeper in the acyl chains. This suggests that it would not be favorable for this compound to cross from one hemilayer to the other in a bilayer system, as was confirmed by our simulations of a DPPC bilayer in the presence of fipronil (unpublished results).

As expected, the free energy for transferring a fipronil molecule from water to the monolayer in the LE phase is more favorable than transferring it to a more condensed monolayer, given that the interactions between the phospholipids are stronger in the latter case. The fact that the penetration of fipronil in the LC phase is still thermodynamically favorable is in accordance to the experimental results, considering that the penetration isotherm showed that fipronil is able to partition into the monolayer at surface pressures corresponding to the LC phase. In addition, it coincides with the observation that in  $\pi$ -MMA compression isotherms fipronil seems to remain inside the monolayer until the collapse surface pressure. This was also observed in the unbiased simulations, in which all the fipronil molecules remained partitioned in the most condensed system studied.

Furthermore, in the experimental isotherms it was observed that fipronil favors the LE phase of DPPC, given that the phase transition to the LC phase begins at higher surface pressures when fipronil is located inside the monolayer. The PMF profiles showed that fipronil partition into the LE phase is more favorable than the partition into the LC phase. If we consider the two systems, LE and LC in the presence of fipronil, the first system resides in an energetic minimum with respect to the latter. So, the energetic cost of transitioning from one phase to the other one would be higher in these systems than in the pure DPPC monolayer.

## 4. Conclusions

In the present work, we analyzed the effects of the insecticide fipronil on the physical properties of phospholipid monolayers. The analysis of the interaction of fipronil with these membrane models can contribute to the characterization of its mode of action. This work was conducted by using a combined experimental and theoretical-computational approach. The experimental results were contrasted with MD simulations in order to provide a molecular insight into the behavior of the system.

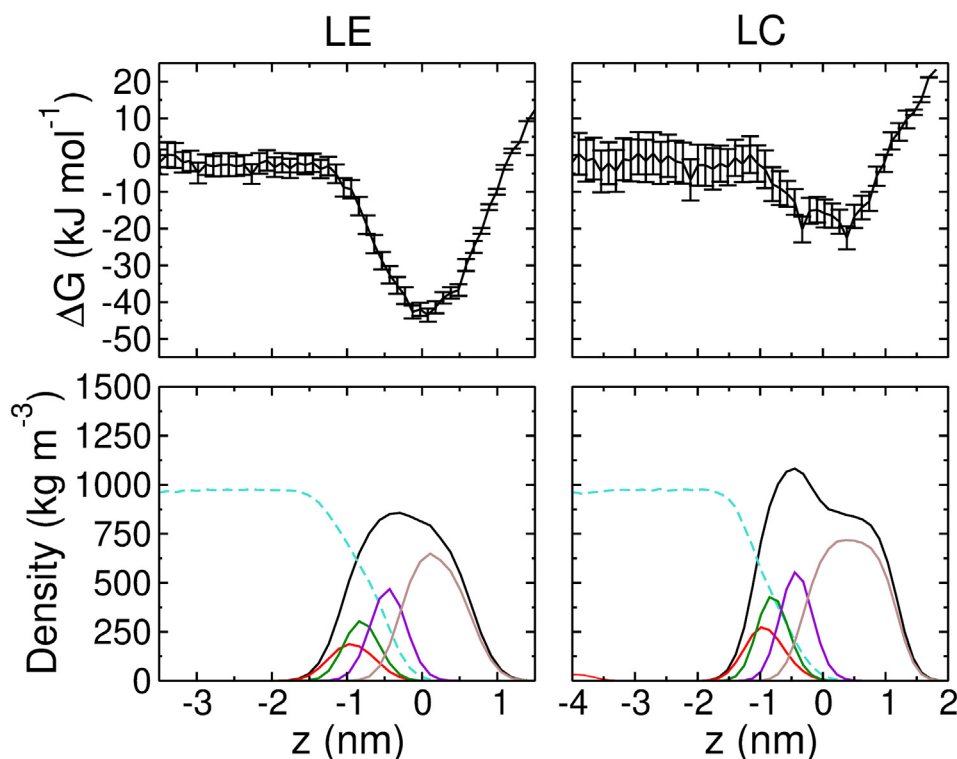


**Fig. 10.** (Upper panels) Free energy profiles for the penetration of fipronil into DPPC monolayers. LE (left) and the LC (right) phases. (Lower panels) Density profiles of the LE and LC systems. DPPC (black lines), water (turquoise dashed line), DPPC acyl chain (brown line), DPPC glycerol group (violet line), DPPC phosphate group (green line) and DPPC choline group (red line). The zero of the z-axis is located in the middle of the monolayer. (For interpretation of the references to color in this figure legend, the reader is referred to the web version of this article.)

Langmuir compression isotherms showed that fipronil molecules produce an expansion in the DPPC isotherm, by acting as spacers between the phospholipids. Also, the partition of fipronil molecules into the lipidic phase affects the characteristic DPPC phase transition, making it to occur at higher surface pressure values and changing the shape of LC domains, as observed by BAM. We were also able to observe an expansion of the simulated DPPC compression isotherm in the presence of fipronil. It is important to consider that only a few previous works have examined the effect of drugs on the compression isotherm of phospholipid monolayers by means of MD simulations, and less of them have been able to contrast them with experimental data.

MD simulations were conducted in such a way that they resemble the behavior of the experimental compression isotherm in the presence of fipronil in the aqueous subphase. Fipronil molecules partitioned into a pre-equilibrated expanded DPPC monolayer and the resulting configuration was simulated in successive more compressed packing states. The analysis of these simulations indicated that fipronil locates in the interphase between the glycerol region and the acyl chains of DPPC. In the LE-LC and in the LC phases, fipronil induces an ordering effect in the acyl chains and a consequent increase in the monolayer thickness, which could be related to the higher experimental surface potential obtained for the DPPC isotherm in the presence of fipronil. The insecticide establishes hydrogen bonds with the carboxylic oxygens of glycerol, and to a lesser extent, with the phosphate group. The most preferable orientation of fipronil would be parallel to the plane of the monolayer.

Free energy profiles obtained from PMF calculations indicated that the partition of fipronil into the phospholipid monolayers is thermodynamically favorable. As expected, the partition is more favorable in the LE phase ( $\sim -45 \text{ kJ}\cdot\text{mol}^{-1}$ ) than in the LC phase ( $\sim -20 \text{ kJ}\cdot\text{mol}^{-1}$ ). However, it is remarkable that, in agreement with the experimental results, the partition into the more condensed packing state is still energetically favorable.

It has been postulated that hydrophobic ligands, in order to reach their active site in a membrane-bound functional protein, first segregate within the lipid bilayer. Subsequently, they undergo fast lateral diffusion and engage in a productive interaction with their biological target

site [80]. Being fipronil a highly lipophilic compound whose target is an intrinsic membrane protein (GABA<sub>A</sub>-R), our results suggest that it could reach its recognition site in the receptor by accumulation and distribution through the bilayer membrane.

Finally, considering the ability of fipronil to interact and to change the physical properties of model membranes, it can be hypothesized that it could modulate the supramolecular organization of biological membranes and consequently the membrane proteins functionality, contributing at least in part to its action mechanism.

#### Credit authorship contribution statement

**Iván Felsztyna:** Conceptualization, Methodology, Validation, Formal analysis, Investigation, Writing - original draft, Writing - review & editing. **Mariela E. Sánchez-Borzone:** Conceptualization, Methodology, Validation, Investigation, Resources, Writing - review & editing, Funding acquisition. **Virginia Miguel:** Conceptualization, Methodology, Formal analysis, Resources, Writing - review & editing, Supervision, Project administration, Funding acquisition. **Daniel A. García:** Conceptualization, Methodology, Resources, Writing - review & editing, Supervision, Project administration, Funding acquisition.

#### Declaration of competing interest

The authors declare that they have no known competing financial interests or personal relationships that could have appeared to influence the work reported in this paper.

#### Acknowledgments

The authors thank Pablo Huais for his assistance in statistical calculations from MD simulations. This work was supported by grants from SECyT-UNC, FONCYT-MINCYT-Argentina (1392-2017), MINCYT-Córdoba and CONICET-Argentina (11220130100075CO). I.F. is a doctoral fellow of CONICET. V.M., M.S.-B. and D.A.G. are Scientific

Research Career members of CONICET. This work used computational resources from CCAD-Universidad Nacional de Córdoba (<http://ccad.unc.edu.ar/>), in particular the Mendieta Cluster, which is part of SNCAD – MINCYT, Argentina.

## Appendix A. Supplementary data

Supplementary data to this article can be found online at <https://doi.org/10.1016/j.bbamem.2020.183378>.

## References

- [1] C.C. Tingle, J.A. Rother, C.F. Dewhurst, S. Lauer, W.J. King, Fipronil: environmental fate, ecotoxicology, and human health concerns, *Reviews of Environmental Contamination and Toxicology*, Springer, 2003, pp. 1–66 Place Published.
- [2] F. Colliot, K. Kukorowski, D. Hawkins, D. Roberts, Fipronil: A New Soil and Foliar Broad Spectrum Insecticide, Brighton Crop Protection Conference-Pests and Diseases, British Crop Protection Council, 1992.
- [3] D.B. Gant, A.E. Chalmers, M.A. Wolff, H.B. Hoffman, D.F. Bushey, Fipronil: action at the GABA receptor, *Rev. Toxicol.* 2 (1998) 147–156.
- [4] A. Nistri, A. Constanti, Pharmacological characterization of different types of GABA and glutamate receptors in vertebrates and invertebrates, *Prog. Neurobiol.* 13 (1979) 117–235.
- [5] W. Sieghart, Allosteric Modulation of GABA<sub>A</sub> Receptors Via Multiple Drug-Binding Sites, Elsevier, Place Published, *Advances in Pharmacology*, 2015, pp. 53–96.
- [6] L. Chen, K.A. Durkin, J.E. Casida, Structural model for  $\gamma$ -aminobutyric acid receptor noncompetitive antagonist binding: widely diverse structures fit the same site, *Proc. Natl. Acad. Sci.* 103 (2006) 5185–5190.
- [7] Y. Ozo,  $\gamma$ -Aminobutyrate-and Glutamate-Gated Chloride Channels as Targets of Insecticides, *Advances in Insect Physiology*, Elsevier, Place Published, 2013, pp. 211–286.
- [8] M. Pytel, K. Mercik, J.W. Mozrzymas, Interaction between cyclodextrin and neuronal membrane results in modulation of GABA<sub>A</sub> receptor conformational transitions, *Br. J. Pharmacol.* 148 (2006) 413.
- [9] R. Sogaard, T.M. Werge, C. Bertelsen, C. Lundbye, K.L. Madsen, C.H. Nielsen, J.A. Lundbæk, GABA<sub>A</sub> receptor function is regulated by lipid bilayer elasticity, *Biochemistry* 45 (2006) 13118–13129.
- [10] D.A. García, S. Quiroga, M.A. Perillo, Flunitrazepam partitioning into natural membranes increases surface curvature and alters cellular morphology, *Chem. Biol. Interact.* 129 (2000) 263–277.
- [11] M.E. Sánchez, A.V. Turina, D.A. García, M.V. Nolan, M.A. Perillo, Surface activity of thymol: implications for an eventual pharmacological activity, *Colloids Surf. B: Biointerfaces* 34 (2004) 77–86.
- [12] G.N. Reiner, M.A. Perillo, D.A. García, Effects of propofol and other GABAergic phenols on membrane molecular organization, *Colloids Surf. B: Biointerfaces* 101 (2013) 61–67.
- [13] M.E. Mariani, M.E. Sánchez-Borzone, D.A. García, Effects of bioactive monoterpene ketones on membrane organization. A langmuir film study, *Chem. Phys. Lipids* 198 (2016) 39–45.
- [14] M.E. Sánchez-Borzone, M.E. Mariani, V. Miguel, R.M. Gleiser, B. Odhav, K.N. Venugopala, D.A. García, Membrane effects of dihydropyrimidine analogues with larvicidal activity, *Colloids Surf. B: Biointerfaces* 150 (2017) 106–113.
- [15] V. Miguel, M.E. Sanchez-Borzone, D.A. García, Interaction of gabaergic ketones with model membranes: a molecular dynamics and experimental approach, *Biochim. Biophys. Acta Biomembr.* 1860 (2018) 1563–1570.
- [16] V. Miguel, M.A. Villarreal, D.A. García, Effects of GABAergic phenols on the dynamic and structure of lipid bilayers: a molecular dynamic simulation approach, *PLoS One* 14 (2019) e0218042.
- [17] G.M. Omann, J.R. Lakowicz, Interactions of chlorinated hydrocarbon insecticides with membranes, *Biochim. Biophys. Acta Biomembr.* 684 (1982) 83–95.
- [18] M.C. Antunes-Madeira, V.M. Madeira, Partition of lindane in synthetic and native membranes, *Biochim. Biophys. Acta Biomembr.* 820 (1985) 165–172.
- [19] M. Suwalsky, C. Rodríguez, F. Villena, F. Aguilar, C.P. Sotomayor, The organochlorine pesticide lindane interacts with the human erythrocyte membrane, *Pestic. Biochem. Physiol.* 62 (1998) 87–95.
- [20] J.M. Bonmatin, C. Giorio, V. Girolami, D. Goulson, D.P. Kreutzweiser, C. Krupke, M. Liess, E. Long, M. Marzaro, E.A.D. Mitchell, Environmental fate and exposure; neonicotinoids and fipronil, *Environ. Sci. Pollut. Res.* 22 (2015) 35–67.
- [21] A.S. Gunasekara, T. Truong, K.S. Goh, F. Spurlock, R.S. Tjeerdema, Environmental fate and toxicology of fipronil, *J. Pestic. Sci.* 32 (2007) 189.
- [22] N. Zheng, J. Cheng, W. Zhang, W. Li, X. Shao, Z. Xu, X. Xu, Z. Li, Binding difference of fipronil with GABA<sub>A</sub>Rs in fruitfly and zebrafish: insights from homology modeling, docking, and molecular dynamics simulation studies, *J. Agric. Food Chem.* 62 (2014) 10646–10653.
- [23] J. Cheng, X.-L. Ju, X.-Y. Chen, G.-Y. Liu, Homology modeling of human  $\alpha 1\beta 2\gamma 2$  and house fly  $\beta 3$  GABA receptor channels and Surflex-docking of fipronil, *J. Mol. Model.* 15 (2009) 1145–1153.
- [24] B. Zhang, L. Zhang, L. He, X. Yang, Y. Shi, S. Liao, S. Yang, J. Cheng, T. Ren, Interactions of fipronil within fish and insects: experimental and molecular modeling studies, *J. Agric. Food Chem.* 66 (2018) 5756–5761.
- [25] S. Ci, T. Ren, Z. Su, Modeling the interaction of fipronil-related non-competitive antagonists with the GABA  $\beta 3$ -receptor, *J. Mol. Model.* 13 (2007) 457.
- [26] S. Feng, Interpretation of mechanochemical properties of lipid bilayer vesicles from the equation of state or pressure–area measurement of the monolayer at the air–water or oil–water interface, *Langmuir* 15 (1999) 998–1010.
- [27] R. Demel, Monolayers-description of use and interaction, *Methods in Enzymology*, Elsevier, 1974, pp. 539–544 Place Published.
- [28] C. Böhm, H. Möhwald, L. Leiserowitz, J. Als-Nielsen, K. Kjaer, Influence of chirality on the structure of phospholipid monolayers, *Biophys. J.* 64 (1993) 553.
- [29] J. Klug, D. Masone, M.G. Del Pópolo, Molecular-level insight into the binding of arginine to a zwitterionic Langmuir monolayer, *RSC Adv.* 7 (2017) 30862–30869.
- [30] D. Mohammad-Aghaie, E. Mace, C.A. Sennoga, J.M. Seddon, F. Bresme, Molecular dynamics simulations of liquid condensed to liquid expanded transitions in DPPC monolayers, *J. Phys. Chem. B* 114 (2009) 1325–1335.
- [31] W. Lin, A.J. Clark, F. Paesani, Effects of surface pressure on the properties of Langmuir monolayers and interfacial water at the air–water interface, *Langmuir* 31 (2015) 2147–2156.
- [32] S.L. Duncan, R.G. Larson, Comparing experimental and simulated pressure-area isotherms for DPPC, *Biophys. J.* 94 (2008) 2965–2986.
- [33] D. Rose, J. Rendell, D. Lee, K. Nag, V. Booth, Molecular dynamics simulations of lung surfactant lipid monolayers, *Biophys. Chem.* 138 (2008) 67–77.
- [34] A. Olżyńska, M. Zubeck, M. Roeselova, J. Korchowiec, L. Cwiklik, Mixed DPPC/POPC monolayers: all-atom molecular dynamics simulations and Langmuir monolayer experiments, *Biochim. Biophys. Acta Biomembr.* 1858 (2016) 3120–3130.
- [35] M. Pickholz, O.N. Oliveira Jr., M.S. Skaf, Interactions of chlorpromazine with phospholipid monolayers: effects of the ionization state of the drug, *Biophys. Chem.* 125 (2007) 425–434.
- [36] M.F. Martini, E.A. Disalvo, M. Pickholz, Nicotinamide and picolinamide in phospholipid monolayers, *Int. J. Quantum Chem.* 112 (2012) 3289–3295.
- [37] A. Skibinsky, R.M. Venable, R.W. Pastor, A molecular dynamics study of the response of lipid bilayers and monolayers to trehalose, *Biophys. J.* 89 (2005) 4111–4121.
- [38] S.K. Kandasamy, R.G. Larson, Molecular dynamics study of the lung surfactant peptide SP-B1–25 with DPPC monolayers: insights into interactions and peptide position and orientation, *Biophys. J.* 88 (2005) 1577–1592.
- [39] J.A. Freitas, Y. Choi, D.J. Tobias, Molecular dynamics simulations of a pulmonary surfactant protein B peptide in a lipid monolayer, *Biophys. J.* 84 (2003) 2169–2180.
- [40] J.J. Giner Casares, L. Camacho, M.T. Martín-Romero, J.J. López Cascales, Effect of Na<sup>+</sup> and Ca<sup>2+</sup> ions on a lipid Langmuir monolayer: an atomistic description by molecular dynamics simulations, *ChemPhysChem* 9 (2008) 2538–2543.
- [41] R. Verger, G.H. De Haas, Enzyme reactions in a membrane model I: a new technique to study enzyme reactions in monolayers, *Chem. Phys. Lipids* 10 (1973) 127–136.
- [42] H. Brockman, Dipole potential of lipid membranes, *Chem. Phys. Lipids* 73 (1994) 57–79.
- [43] M. Kodama, O. Shibata, S. Nakamura, S. Lee, G. Sugihara, A monolayer study on three binary mixed systems of dipalmitoyl phosphatidyl choline with cholesterol, cholestanol and stigmaterol, *Colloids Surf. B: Biointerfaces* 33 (2004) 211–226.
- [44] C.A. Schneider, W.S. Rasband, K.W. Eliceiri, NIH image to ImageJ: 25 years of image analysis, *Nat. Methods* 9 (2012) 671.
- [45] M.J. Abraham, T. Murtola, R. Schulz, S. Páll, J.C. Smith, B. Hess, E. Lindahl, GROMACS: high performance molecular simulations through multi-level parallelism from laptops to supercomputers, *SoftwareX* 1 (2015) 19–25.
- [46] J.P.M. Jämbeck, A.P. Lyubartsev, Derivation and systematic validation of a refined all-atom force field for phosphatidylcholine lipids, *J. Phys. Chem. B* 116 (2012) 3164–3179.
- [47] W.L. Jorgensen, J. Chandrasekhar, J.D. Madura, R.W. Impey, M.L. Klein, Comparison of simple potential functions for simulating liquid water, *J. Chem. Phys.* 79 (1983) 926–935.
- [48] V. Miguel, M.E. Defonsi Lestard, M.E. Tuttolomondo, S.B. Díaz, A. Ben Altabet, M. Puiatti, A.B. Pierini, Molecular view of the interaction of S-methyl methanethiosulfonate with DPPC bilayer, *Biochim. Biophys. Acta Biomembr.* 1858 (2016) 38–46.
- [49] M. Frisch, G. Trucks, H. Schlegel, G. Scuseria, M. Robb, J. Cheeseman, J. Montgomery Jr., T. Vreven, K. Kudin, J. Burant, Gaussian 03, Revision c. 02, Gaussian, Inc, Wallingford, CT, 2004, p. 4.
- [50] J. Wang, R.M. Wolf, J.W. Caldwell, P.A. Kollman, D.A. Case, Development and testing of a general amber force field, *J. Comput. Chem.* 25 (2004) 1157–1174.
- [51] A.W. Sousa da Silva, W.F. Vranken, ACPYPE—antechamber python parser interface, *BMC Res. Notes* 5 (2012) 367.
- [52] L. Martínez, R. Andrade, E.G. Birgin, J.M. Martínez, PACKMOL: a package for building initial configurations for molecular dynamics simulations, *J. Comput. Chem.* 30 (2009) 2157–2164.
- [53] S.E. Feller, Y. Zhang, R.W. Pastor, Computer simulation of liquid/liquid interfaces. II. Surface tension-area dependence of a bilayer and monolayer, *J. Chem. Phys.* 103 (1995) 10267–10276.
- [54] Y. Zhang, S.E. Feller, B.R. Brooks, R.W. Pastor, Computer simulation of liquid/liquid interfaces. I. Theory and application to octane/water, *J. Chem. Phys.* 103 (1995) 10252–10266.
- [55] C. Vega, E. De Miguel, Surface tension of the most popular models of water by using the test-area simulation method, *J. Chem. Phys.* 126 (2007) 154707.
- [56] H.J.C. Berendsen, J.P.M. Postma, W.F. van Gunsteren, A. DiNola, J.R. Haak, Molecular dynamics with coupling to an external bath, *J. Chem. Phys.* 81 (1984) 3684–3690.
- [57] U. Essmann, L. Perera, M.L. Berkowitz, T. Darden, L. Hsing, L.G. Pedersen, A smooth particle mesh Ewald method, *J. Chem. Phys.* 103 (1995) 8577–8593.
- [58] S. Kumar, J.M. Rosenberg, D. Bouzida, R.H. Swendsen, P.A. Kollman, The weighted histogram analysis method for free-energy calculations on biomolecules. I. The



- method, *J. Comput. Chem.* 13 (1992) 1011–1021.
- [59] J.S. Hub, B.L. de Groot, D. van der Spoel, g\_wham — a free weighted histogram analysis implementation including robust error and autocorrelation estimates, *J. Chem. Theory Comput.* 6 (2010) 3713–3720.
- [60] W. Humphrey, A. Dalke, K. Schulten, VMD: visual molecular dynamics, *J. Mol. Graph.* 14 (1996) 33–38.
- [61] G.E.G. Gonçalves, F.S. de Souza, J.H.G. Lago, L. Caseli, The interaction of eugenol with cell membrane models at the air–water interface is modulated by the lipid monolayer composition, *Biophys. Chem.* 207 (2015) 7–12.
- [62] P. Toimil, G. Prieto, J. Miñones Jr, F. Sarmiento, A comparative study of F-DPPC/DPPC mixed monolayers. Influence of subphase temperature on F-DPPC and DPPC monolayers, *Phys. Chem. Chem. Phys.* 12 (2010) 13323–13332.
- [63] V.L. Shapovalov, Interaction of DPPC monolayer at air–water interface with hydrophobic ions, *Thin Solid Films* 327 (1998) 599–602.
- [64] J.V.N. Ferreira, T.M. Capello, L.J.A. Siqueira, J.H.G. Lago, L. Caseli, Mechanism of action of thymol on cell membranes investigated through lipid Langmuir monolayers at the air–water interface and molecular simulation, *Langmuir* 32 (2016) 3234–3241.
- [65] C.B. Casper, D. Verreault, E.M. Adams, W. Hua, H.C. Allen, Surface potential of DPPC monolayers on concentrated aqueous salt solutions, *J. Phys. Chem. B* 120 (2016) 2043–2052.
- [66] J.V.N. Ferreira, S.d.S. Grecco, J.H.G. Lago, L. Caseli, Ultrathin films of lipids to investigate the action of a flavonoid with cell membrane models, *Mater. Sci. Eng. C* 48 (2015) 112–117.
- [67] NIH, [Pubchem](#), 2020.
- [68] T.E. Goto, L. Caseli, The interaction of mefloquine hydrochloride with cell membrane models at the air–water interface is modulated by the monolayer lipid composition, *J. Colloid Interface Sci.* 431 (2014) 24–30.
- [69] R. Maget-Dana, The monolayer technique: a potent tool for studying the interfacial properties of antimicrobial and membrane-lytic peptides and their interactions with lipid membranes, *Biochim. Biophys. Acta Biomembr.* 1462 (1999) 109–140.
- [70] R.A. Demel, W.S.M. Geurts Van Kessel, R.F.A. Zwaal, B. Roelofsen, L.M. Van Deenen, Relation between various phospholipase actions on human red cell membranes and the interfacial phospholipid pressure in monolayers, *Biochim. Biophys. Acta Biomembr.* 406 (1975) 97–107.
- [71] D. Marsh, Lateral pressure in membranes, *Biochim. Biophys. Acta Biomembr.* 1286 (1996) 183–223.
- [72] P. Krüger, M. Lösche, Molecular chirality and domain shapes in lipid monolayers on aqueous surfaces, *Phys. Rev. E* 62 (2000) 7031.
- [73] N. Nandi, K. Thirumoorthy, D. Vollhardt, Chiral discrimination in stearyl amine glycerol monolayers, *Langmuir* 24 (2008) 9489–9494.
- [74] K. Thirumoorthy, N. Nandi, D. Vollhardt, Role of electrostatic interactions for the domain shapes of Langmuir monolayers of monoglycerol amphiphiles, *J. Phys. Chem. B* 109 (2005) 10820–10829.
- [75] L. Huynh, N. Perrot, V. Beswick, V.r. Rosilio, P.A. Curmi, A. Sanson, N. Jamin, Structural properties of POPC monolayers under lateral compression: computer simulations analysis, *Langmuir* 30 (2014) 564–573.
- [76] M. Javanainen, A. Lamberg, L. Cwiklik, I. Vattulainen, O.S. Olila, Atomistic model for nearly quantitative simulations of Langmuir monolayers, *Langmuir* 34 (2018) 2565–2572.
- [77] D. Lopes, S. Jakobtorweihen, C. Nunes, B. Sarmiento, S. Reis, Shedding light on the puzzle of drug-membrane interactions: experimental techniques and molecular dynamics simulations, *Prog. Lipid Res.* 65 (2017) 24–44.
- [78] S.O. Nielsen, C.F. Lopez, P.B. Moore, J.C. Shelley, M.L. Klein, Molecular dynamics investigations of lipid Langmuir monolayers using a coarse-grain model, *J. Phys. Chem. B* 107 (2003) 13911–13917.
- [79] R.J. Demchak, T. Fort Jr, Surface dipole moments of close-packed un-ionized monolayers at the air–water interface, *J. Colloid Interface Sci.*, 46 (1974) 191–202.
- [80] A. Makriyannis, X. Tian, J. Guo, How lipophilic cannabinergic ligands reach their receptor sites, *Prostaglandins Other Lipid Mediat.* 77 (2005) 210–218.